Preprint, published in AIAA Journal, 55(1), 332-338, 2017. http://dx.doi.org/10.2514/1.J054897

Effects of Shock-Tube Cleanliness on Slender-Body Hypersonic Instability and Transition Studies at High Enthalpy

Joseph S. Jewell*

Air Force Research Laboratory, Wright-Patterson AFB, OH 45433, USA

Nicholaus J. Parziale†

Stevens Institute of Technology, Hoboken, NJ 07030, USA

Ivett A. Leyva‡

Air Force Office of Scientific Research, Arlington AFB, VA 22203, USA

Joseph E. Shepherd§

California Institute of Technology, Pasadena, CA 91125, USA

I. Introduction

The prediction of high-speed boundary-layer transition (BLT) location is critical to hypersonic vehicle design; this is because increased skin friction and surface heating rate after transition result in increased weight of the thermal protection system (TPS). Experimental studies using hypervelocity wind tunnels are one component of BLT research.

The free-stream disturbances in supersonic and hypersonic wind tunnels include acoustic waves, entropy inhomogeneity, and vortical perturbations, in addition to microscale and macroscale particles [1]. These disturbances, in whatever form, can significantly influence boundary layer instability and transition-location measurements such that confidence in the experimental measurements

*Research Aerospace Engineer (NRC Research Associate), AFRL/RQHF, Wright-Patterson AFB, OH 45433. AIAA Senior Member. jjewell@alumni.caltech.edu

†Assistant Professor, Mechanical Engineering, Castle Point on Hudson, Hoboken, NJ 07030. AIAA Member.

‡Program Officer, AFOSR/RTE, Arlington AFB, VA 22203. AIAA Associate Fellow.

§Professor, Graduate Aeronautical Laboratories, 1200 E. California Blvd., MC 105-50, Pasadena, CA 91125. AIAA Senior Member.

is compromised. For this reason, transition researchers have made extensive efforts in minimizing and characterizing free-stream disturbance levels.

Hypersonic wind tunnels exist where there are low disturbance levels, such as those at Purdue [2–4] and Texas A&M [5, 6]. Currently, the parameter space available to low-disturbance hypersonic wind tunnels does not permit the study of the interaction of boundary-layer instability and thermo-chemistry, which is important for accurately modeling realistic reentry flows; this is because low-disturbance hypersonic tunnels have a low ordered kinetic energy, or total enthalpy, in the free-stream relative to relevant chemical or vibrational energy levels.

To study the effects of thermo-chemistry on BLT in ground-test, the total enthalpy of the flow must be sufficiently high. One such ground-test facility to generate "high-enthalpy" flows is the reflected-shock tunnel. In the past, researchers have used shock tunnels and reflected-shock tunnels to study BLT [7–13]. More recently, in the HEG reflected-shock tunnel, Laurence et al. [14–16] report a schlieren-based technique for the investigation of disturbances in hypervelocity boundary layers. In those reports, high-resolution and time-resolved images of the second-mode instability of a hypervelocity boundary layer on a slender cone data are presented. At Caltech in the T5 reflected-shock tunnel, Germain and Hornung [17], Adam and Hornung [18], Rasheed et al. [19], Jewell et al. [20], and Parziale et al. [21] studied hypervelocity BLT on a slender cone; those researchers performed approximately 1000 experiments and made significant progress in developing visualization and direct measurement techniques. These diagnostic advances made possible the investigation of high-enthalpy effects on BLT in different gases and hypervelocity BLT control by porous coatings. However, special attention to potential particulate contamination in high-enthalpy impulse facilities is required, relative to conventional "cold" hypersonic tunnels, because of the harsh conditions in the facility before and after the test flow over the model.

To reduce the effects of particulates of BLT on slender cones [20, 21, 23–27], we devised a new cleaning and fill procedure for the shock tunnel, which is the subject of this paper. Possible sources of particles include piston buffer material, piston brakes, test gas impurities, and the mylar secondary diaphragm. In particular, Parziale et al. [25] noted that experiments performed immediately after an experiment where the piston buffers shattered had less predictable noise profiles.

With stringent cleaning of the shock tube, it is possible to mitigate particulate contamination and repeatably obtain transition at specified locations through a careful selection of reservoir conditions.

Analyses of the current data with standard linear stability methods indicates that the transition location corresponds to second-mode amplification factors e^N with $N \approx 8$–12 at transition onset [20, 26]. These values, even those obtained prior to implementation of the cleaning regimen, are high compared to the more typical values of $N \approx 5$–6 usually characterizing a "noisy" tunnel [2]. Although the transition N factors recorded early in the current test campaign were higher than expected for a "noisy" tunnel, there was a larger than desired scatter in results. One reason for a higher transition N factor for the current data may be the mismatch between freestream noise spectrum and boundary layer unstable frequencies for second-mode disturbances, while the relatively large scatter may result from particulate-induced bypass transition affecting some experiments. Parziale et al. [25] found that noise in the T5 free stream is relatively low-frequency compared with the most unstable boundary-layer frequencies. This hypothesis is implicitly supported by the recent analysis of Gronvall et al. [28] who found a transition onset value of $N \approx 8$ for the experiments of Tanno et al. [12], which were also performed in a reflected-shock tunnel, although at lower enthalpy than the present study, and for a limited range of conditions, with unspecified cleaning procedures. At the start of the present test campaign, prior to the implementation of the cleaning regimen, we encountered difficulty in achieving repeatable transition Reynolds numbers and N factors. Our hypothesis was that bypass transition was caused sporadically by particulate leftover from prior experiments; thus, it became a focus to reduce particulate.

Recently, Fedorov [22] has examined receptivity to particulate-laden flows, modeling the particulates as spherical solids impacting the supersonic boundary layer, and making numerical estimates for particulate-driven transition onset for various sizes and densities. Fedorov found that both the N-factor and the transition Reynolds number were strongly influenced by particle characteristics, including size and number density. For computations with a 14-degree half-angle sharp wedge at Mach 4 in the standard atmosphere at 20 km, transition onset N-factor dropped from 12 for particles of radius 5 μm to 7 for particles of radius 50 μm; this provides the motivation to

minimize particulates in the free stream is apparent for ground tests of BLT in impulse facilities.

Examples of data from experiments before and after the cleaning regimen was instituted are presented, and these results are compared. Then, a statistical analysis of transition Reynolds number is presented to quantify the change in repeatability of the experiment.

II. Facility

All measurements are made in T5, the free-piston driven reflected-shock tunnel at the California Institute of Technology. T5 is designed to simulate flow conditions and aerodynamics of hypervelocity vehicles at total enthalpies up to 25 MJ/kg and freestream velocities of up to 6000 m/s. During each T5 experiment, a piston-compressed He/Ar driver ruptures a scored, stainless steel primary diaphragm. Following the primary diaphragm rupture, a shock wave propagates in the shock tube, is reflected off the end wall breaking the secondary diaphragm, and re-processes the test gas, which is then expanded through a converging-diverging contoured nozzle to ~Mach 5.5 in the test section. [24, 26, 29].

Measured primary shock speed and reservoir pressure are used to compute the reservoir conditions for each test. Thermo-chemical equilibrium calculations are performed using Cantera [30] with the Shock and Detonation Toolbox [31] using thermodynamic data are found valid for the high temperature conditions in T5 [32, 33]. The test gas reaches its highest temperature in the stagnation region. For the 74 tests comprising the present data set, the calculated reservoir temperature ranged from 3380 K to 6930 K, with the mean and median both 5510 K. The cone mean flow is computed with the STABL software suite, as described by Johnson [34] and Johnson et al. [35] and recently applied by Wagnild [36]. Boundary-layer profiles and edge properties are extracted from the mean flow solutions during post-processing.

III. Shock Tube Fill Gas Quality and Cleaning Procedure

Experience with testing in T5 revealed an opportunity to increase the quality of the flow over the model. Improvement was achieved by using higher quality gas to fill the shock tube and cleaning the shock tube more thoroughly between experiments. The most repeatable results were obtained

with the “ALPHAGAZ” grade of Air Liquide products[a].

Even after changing to research quality test gas, we found it difficult to repeatably specify a transition location with a choice of run conditions. We hypothesized that this was due to the particulates in the shock tube left over from the previous run. However, the lack of a comprehensive test series carried out after changing to higher-quality gas, but before extensive particulate reduction efforts, precludes conclusively separating the effects of higher test gas quality from the effects of the improved cleaning procedure. Experience in other facilities has shown that particulate contamination is very effective at promoting transition [3]. In order to minimize particulates, the cleaning procedure between each operational cycle was changed to: 1) clean the shock-tube end with a Scotch-Brite pad, 2) clean the shock-tube end with acetone on a mop, 3) pass four shop towels rolled into a cylinder and drag them through the shock tube, the outer-most towel being misted with acetone, 4) repeat step 3 until the outermost towel does not become dirty after a pass through the shock tube (as many as 20 times). 5) repeat step 3 with the outer towel misted with isopropyl alcohol to remove any remaining acetone residue. The nozzle and nozzle throat are cleaned by hand with Kimwipes using the same sequence of solvents.

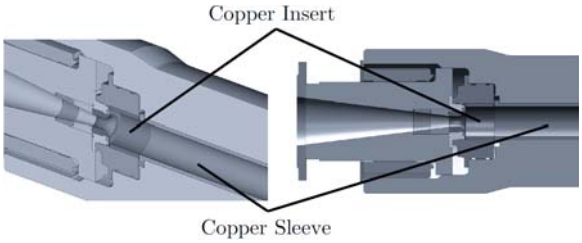

Figure 1. The copper sleeve and insert at the shock tube end.

The region at the end of the shock tube in a reflected-shock tunnel is an additional area of concern with respect to shot-to-shot variation. In T5, this region is comprised of a copper insert and sleeve, shown in a detail view as Fig. 1. Taylor and Hornung [37] note that wall roughness in the reflected-shock region can increase the shock bifurcation asymptotic height, which is the distance above the side wall within which wall effects are important behind a reflected shock wave. This behavior is undesirable because of the induced non-uniformity of the reservoir gas and

[a]The relative O_2 to N_2 balance for ALPHAGAZ air is tighter (±0.5% by partial pressure) than lower-grade gas, and the total hydrocarbons are specified to be less than 0.05 ppm.

decreased test time due to driver gas contamination of the reservoir gas [38].

After completing the cleaning, the copper insert and copper sleeve had a smooth finish. The roughness of the 90 mm diameter shock tube is estimated to be less than 25 µm. Throughout the test campaign the copper insert and sleeve were maintained in this condition to avoid the detrimental effects of shock bifurcation as much as possible.

IV. FLDI and Heat-Flux Measurements Examples, With and Without Cleaning

In this section we present two examples of heat-flux and FLDI data: experiment 2769 performed with the cleaning procedure explained in this paper and experiment 2702 performed without adequately cleaning T5.

The focused laser differential interferometry (FLDI) is an optical technique, developed by Smeets [39], and recently used in T5 [21, 27], which permits the high-speed and non-intrusive interrogation of small-amplitude density perturbations within a small sensitive region of the beam path, while rejecting perturbations outside of the sensitive region, including those resulting from the nozzle shear layer. The effect of cleaning on transition location and repeatability was examined in a series of tests using the FLDI to measure disturbances within the boundary on a 5-degree half-angle smooth cone at zero angle of attack. The FLDI was located at a fixed point relative to the cone and the reservoir conditions were changed to adjust the Reynolds number at the FLDI probe volume. Previous test data and numerical simulations of tunnel performance enable carrying out testing at specified Reynolds numbers and total enthalpy. For conditions with sufficiently low Reynolds number, laminar response would be expected based on past heat-flux measurements. However, in some instances where laminar flow was expected, boundary-layer instability measurements revealed that a sporadic and initially inexplicable period of broadband response would pass through the probe volume of the focused laser differential interferometer (FLDI).

To illustrate these events, spectrograms of two runs at similar run conditions are compared in Figs. 2a and 2b. In Fig. 2a, we present a spectrogram of the FLDI data from experiment 2702, which was performed prior to the implementation of the new cleaning procedure. The spectrogram

shows a sporadic and large swath of broad-band response, followed by a period where minimal disturbances are detected, followed by a period of narrowband response. The FLDI data show contrast to data recorded after the new cleaning-procedure implementation; for example, data from experiment 2769. We present a spectrogram for experiment 2769 in Fig. 2b, which shows no broadband response and only a series of narrowband peaks.

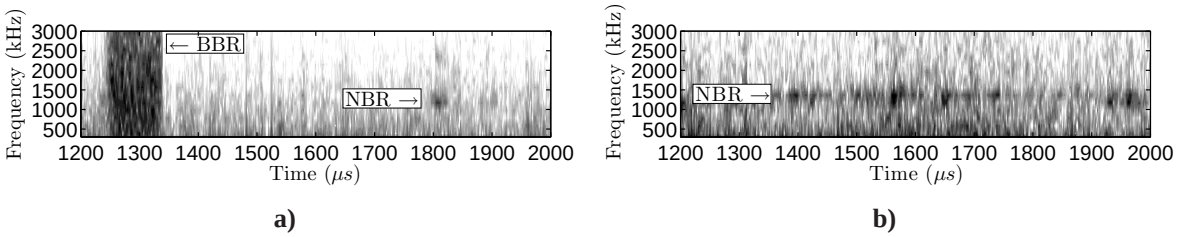

Figure 2. Power spectral density (arbitrary units) of FLDI output as a function of time. Darker shading indicates larger amplitude. BBR is broadband response, NBR is narrowband response. In a, an example of sporadic response shows a large swath of broad-band response, followed by a period where minimal disturbances are detected, followed by a period of narrowband response (test 2702). In b, an example of a stochastic but sensible series of narrowband peaks (test 2769).

The hypersonic quiet tunnel currently represents the state-of-the-art facility class in terms of disturbance environment. Quiet tunnel design and operation includes careful particulate mitigation, which is partially motivated by preserving the mirror-like finish on the nozzle wall necessary to preserve low acoustic disturbance levels by preventing nozzle wall boundary layer transition [40]. The FLDI data in Fig. 2b, recorded after the T5 cleaning procedure was implemented, exhibits narrowband response at distinct frequencies associated with the second mode. This is qualitatively similar to spectrograms of slender-body hypersonic boundary-layer instability obtained in a low-disturbance facility by Hofferth et al. [5].

The FLDI measurements provide detailed spectral data enabling the narrow-band versus broad-band characterization of boundary-layer disturbances; however, this data is limited spatially to the FLDI probe volume. Heat-flux measurements were performed to provide data to assess the effect of cleaning on the entire surface of the model, which enabled the tracking of large turbulent spots suspected to have been caused by particulate in the shock tube prior to running the experiment.

The model is a smooth 5-degree half-angle aluminum cone similar to that used in a number of previous experimental studies in T5, 1 m in length, and is composed of three sections: a nominally sharp tip (radius less than 0.175 mm) fabricated of molybdenum, an interchangeable mid-section

(in the present experiments this section is a smooth, solid piece of plastic), and the main body, which is instrumented with a total of 80 flush-mounted annular thermocouples evenly spaced at 20 lengthwise locations beginning at 221 mm from the tip of the cone, with each row located 38 mm from the last. This sensor spacing corresponds to uncertainty estimates in edge Reynolds number at transition onset from $\pm 9.34 \times 10^4$ to $\pm 4.80 \times 10^5$, and in reference Reynolds number at transition onset from $\pm 6.00 \times 10^4$ to $\pm 3.33 \times 10^5$. Heat flux on the cone was obtained from the thermocouples, which are of a design first used by Sanderson and Sturtevant [41, 42]. These thermocouples have a response time on the order of a few microseconds and have been successfully used for boundary-layer transition onset determination (*i.e.*, the most forward departure of the nondimensionalized heat flux from an appropriate laminar correlation) as more fully described in Adam and Hornung [18], Rasheed et al. [19], and Jewell et al. [20], as well as for tracking the propagation of turbulent spots by Jewell et al. [23]. Time- and spatially-resolved heat flux data allows the presentation of a "movie" of heat flux over the entire instrumented surface of the cone by interpolating the processed thermocouple signals.

In Fig. 3, we present several heat-flux frames from the test time of experiment 2702, which corresponds to the FLDI result shown in Fig. 2a, and was performed prior to the new cleaning-procedure implementation. In addition, Fig. 4 presents several heat flux frames from the test time of experiment 2769, which corresponding to the FLDI result shown in Fig. 2b, and was performed following cleaning-procedure implementation. The boundary-layer edge conditions for these two shots are recorded in Table 1.

In test 2702 with a dirty shock tube, a turbulent spot is observed to propagate downstream, crossing the location of the FLDI sensor at the same time as broadband response is observed in the spectrogram for test 2702 (Fig. 2a and Fig. 3 at $\sim$ 1250 – 1350 µs). This spot is generated independently of the other transition events that are typically observed in natural transition and is therefore believed to be the result of particulate impact on the boundary layer during the test time, following the mechanism outlined by Fedorov [22]. The large amplitude of the FLDI signal correlates with elevated heat transfer as the turbulent spot passes the thermocouples nearest the FLDI sensitive region, as shown in Fig. 5, lending confidence to the conclusion that the FLDI and

heat-flux gauges are measuring the same turbulent spot.

In contrast, in test 2769 with a clean shock tube, no turbulent spots are observed near the FLDI during the test time, although intermittent turbulent flow typical of natural modal transition is observed near the end of the cone. This observation is consistent with the lack of broadband response observed in the spectrogram for test 2769 (Fig. 2b and Fig. 4). The spot in test 2702 is first observed at a location on the cone where stability computations [43] find that N≈ 4, which indicates that it is unlikely to be the result of modal transition, while the natural transition front in test 2759 is observed at a location where N≈ 10.

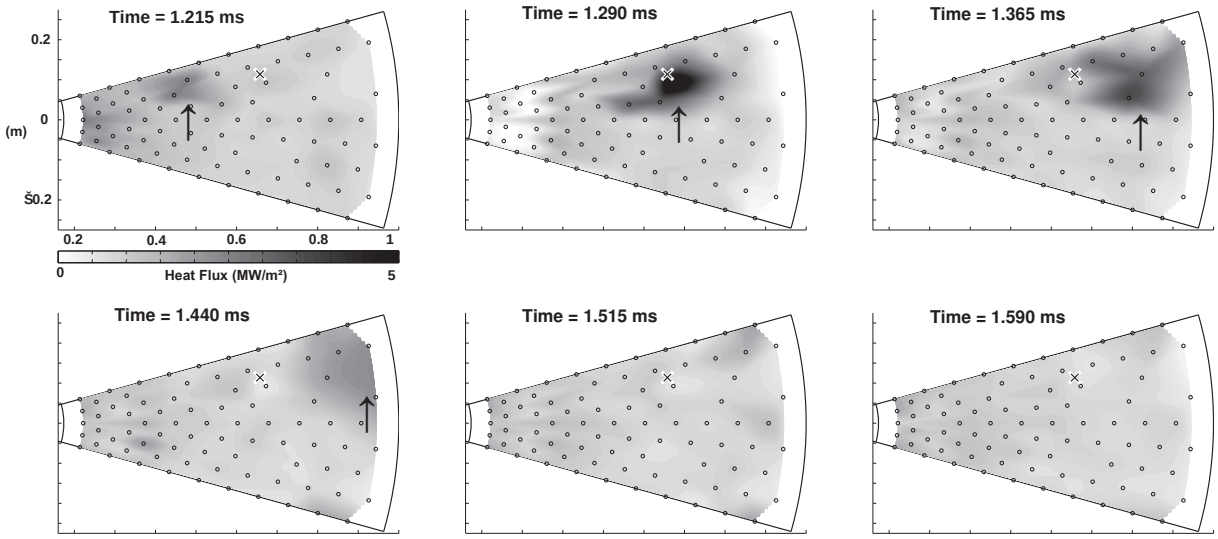

Figure 3. Heat flux spatial distributions from test 2702 at 0.075 ms intervals covering a total time of 0.375 ms, during which a turbulent spot is observed (first frame, top left, marked with an arrow) and propagates downstream and eventually off the end of the cone in the subsequent three frames. The location of the FLDI is marked with an "X" at 665 mm from the tip.

Table 1. Summary of edge conditions for tests 2702 and 2769 in air.

Test	h_{res} (MJ/kg)	P_{res} (MPa)	U_e (m/s)	P_e (kPa)	T_e (K)	Tv_e (K)	ρ_e (kg/m^3)	M_e (-)	unit Re_e (1/m)
2702	8.45	49.9	3680	36.9	1420	1420	0.090	4.84	6.34×10^6
2769	10.5	60.8	4030	47.1	1830	1830	0.092	4.66	6.00×10^6

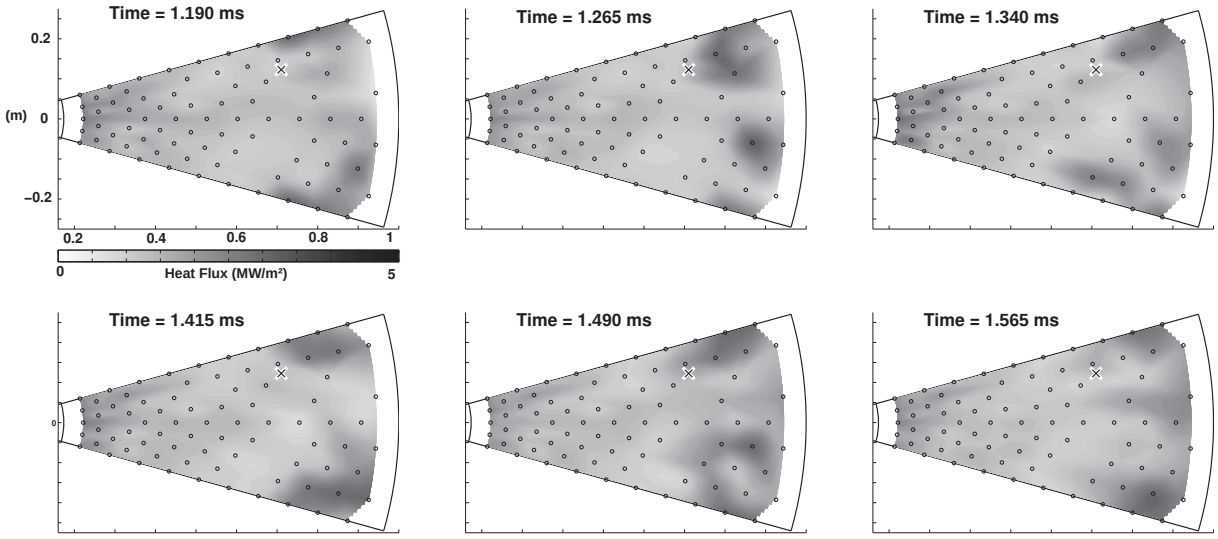

Figure 4. Heat flux spatial distributions from test 2769 at 0.075 ms intervals covering a total time of 0.375 ms. While intermittent turbulent flow is observed near the end of the cone, no propagating turbulent bursts are visible during the experiment. The location of the FLDI is marked with an "X" at 718 mm from the tip.

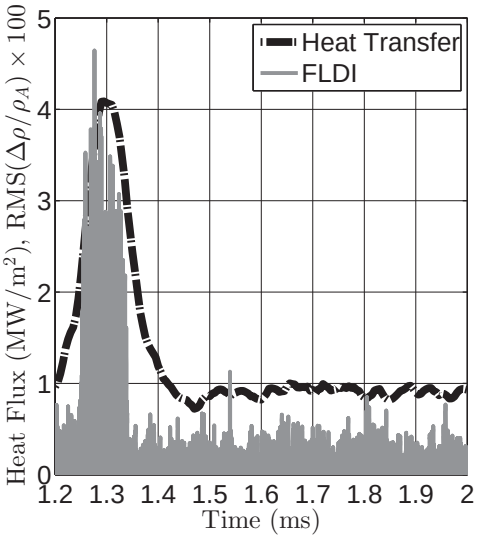

Figure 5. Heat flux signal from test 2702 interpolated from the four thermocouples nearest to the FLDI sensitive region compared to the FLDI signal from the same experiment. A passing turbulent spot at about 1.3 ms causes both elevated local heat transfer and broadband density disturbance.

V. Transition Onset Correlations

To test our hypothesis of tunnel cleaning improving transition location repeatability, we carried out a statistical analysis of a total of 74 tests before ($n = 40$) and after ($n = 34$) improvements in the cleaning regimen. Evidence of correlation between transition location, tunnel parameters, and

tunnel cleanliness is sought using reverse-stepwise regression [44] as implemented in MATLAB [45]. The p-value required to remove a parameter from the regression is 0.1.

The predictor parameters chosen to seek correlation with transition Reynolds numbers are reservoir pressure P_{res}, reservoir enthalpy h_{res}, and x_3, which is a cleaning status indicator variable consisting of a vector of ones and zeros, where 1 and 0 designate an experiment performed before and after the cleaning procedure was implemented, respectively. The three predictor values, as well as the three crossterms are included in the model's initial state. If the cleaning variable, or a crossterm with the cleaning variable, remains in the final model after reverse-stepwise regression, this is a statistically significant indication that the cleaning procedure affects the resulting response variables, which are Re_{Tr} and Re^*_{Tr}. Re_{Tr} and Re^*_{Tr} are the edge Reynolds number at the transition onset location and the Reynolds number evaluated at reference conditions at the transition onset location, respectively. Stepwise regression was performed twice, once with each transition Reynolds number as the response variable.

The reverse-stepwise regression model for Re_{Tr} retained P_{res}, h_{res}, and x_3, and the $P_{\text{res}} \cdot x_3$ and $h_{\text{res}} \cdot x_3$ crossterms, indicating that the null hypothesis of a zero coefficient is rejected for pressure, enthalpy, and tunnel cleanliness. The rearward-stepwise regression model for Re^*_{Tr} retained P_{res}, h_{res} x_3, and the $h_{\text{res}} \cdot x_3$ crossterm, indicating that the null hypothesis of a zero coefficient is rejected for pressure, enthalpy, and tunnel cleanliness. In both cases, pressure and enthalpy crossterm is excluded from the final model, which indicates that reasonable linear models for both transition Reynolds numbers may be constructed using only the pressure and enthalpy parameters if the data are divided into pre-cleaning regimen and post-cleaning regimen data subsets to eliminate the influence of x_3 and the two x_3 crossterms.

The coefficient of determination of correlation between tunnel-parameters and transition Reynolds number was used as a metric of repeatability within each data subset. A higher coefficient of determination indicates higher repeatability. Jewell et al. [26, 46] showed that the tunnel parameters h_{res} (reservoir enthalpy) and P_{res} (reservoir pressure) could be used as predictor variables to construct statistically significant linear models of transition Reynolds number Re_{Tr} for both the present data sets and the historical T5 transition data of Germain and Hornung [17] and Adam and Hor-

nung [18] for air, CO_2, and N_2. In the present work, only air transition data is considered. These linear models take the form:

$$\mathrm{Re}_{\mathrm{Tr}}(P_{\mathrm{res}}, h_{\mathrm{res}}) = \mathrm{Re}_{\mathrm{intercept}} + C_{P_{\mathrm{res}}} P_{\mathrm{res}} + C_{h_{\mathrm{res}}} h_{\mathrm{res}}$$

Here the constant coefficients that define the regression plane, $C_{P_{\mathrm{res}}}$, $C_{h_{\mathrm{res}}}$ and the Re intercept are computed via multivariable-linear regression as implemented in MATLAB. The complete model results for the data acquired before the implementation of new shock tube cleaning procedures are recorded in Table 2, and the results for the data acquired after the implementation of the cleaning procedures are recorded in Table 3. Both the $\mathrm{Re}_{\mathrm{Tr}}$ and $\mathrm{Re}^*_{\mathrm{Tr}}$ models have normally distributed errors, and each set of residuals exhibits limited heteroskedacity.

The position of the best-fit Re plane computed relative to the h_{res}-P_{res} plane (*i.e,* the intercept) is 5.90×10^5 for the dirty tunnel data and 1.83×10^6 for the clean tunnel data. The larger intercept value for the clean results is an indication that the tunnel cleaning procedure tends to increase transition onset Reynolds number. Moreover, the clean tunnel results show less dispersion than the dirty results, which is consistent with the stochastic effect that would be expected in dirty flow from an unknown and probably inconsistent variation in particle size and number density, linear regression analysis performed using the tunnel parameters, reservoir enthalpy (h_{res}) and reservoir pressure (P_{res}), as the predictor variables and the edge Reynolds number at the transition onset location ($\mathrm{Re}_{\mathrm{Tr}}$) as the response variable had a modeled R^2 value of 0.50 for the experiments prior to cleaning procedure implementation, and an R^2 value of 0.80 subsequent to the implementation of the cleaning procedure. When the same regression analysis is performed using the Reynolds number calculated at reference conditions at the transition onset location ($\mathrm{Re}^*_{\mathrm{Tr}}$), $R^2 = 0.70$ prior to cleaning procedure implementation and $R^2 = 0.86$ subsequently.

Transition onset measurements, full details of which are described in Jewell [26] and Jewell and Shepherd [43], were more consistent in experiments after the shock tube cleaning procedures described in Section III were implemented ($n = 34$) than in those prior ($n = 40$). Reservoir temperatures were similar for each subset of the data. The 34 tests after the implementation of the cleaning procedure had calculated reservoir temperatures ranging from 3380 K to 6410 K, with a

median of 5520 K and a mean of 5490 K. The 40 tests prior to the implementation of the cleaning procedure had calculated reservoir temperatures ranging from 4010 K to 6930 K, with a median of 5510 K and a mean of 5520 K.

Table 2. Multivariable linear regression analyses with $\mathbf{Re_{Tr}}$ ($\mathbf{R^2 = 0.50}$) and $\mathbf{Re^*_{Tr}}$ ($\mathbf{R^2 = 0.70}$) as the response variables for "dirty" tunnel results (n = 40) acquired before the implementation of the new cleaning regimen. We use a significance level of 5% (*i.e.*, requiring a *p*-value less than 0.05 to reject the null hypothesis that a given coefficient is zero). The coefficients found to be statistically significant under this criterion are in bold print.

	Re_{Tr}	Re^*_{Tr}
Re intercept	5.90×10^5	$\mathbf{-1.38 \times 10^6}$
p-value	0.37394	0.00834
Standard Error	6.55×10^5	4.95×10^5
$C_{P_{res}}$	$\mathbf{4.82 \times 10^4}$	$\mathbf{3.54 \times 10^4}$
p-value	2.18×10^{-4}	2.99×10^{-4}
Standard Error	1.18×10^4	8.87×10^3
$C_{h_{res}}$	9.18×10^5	$\mathbf{2.98 \times 10^5}$
p-value	0.34578	2.12×10^{-4}
Standard Error	9.61×10^4	7.26×10^4
model *F*-statistic	18.4	43.4
model *p*-value	2.82×10^{-6}	1.99×10^{-10}

VI. Conclusions

We have shown that an improved cleaning procedure in a hypervelocity shock tunnel improves the repeatability of transition measurements, demonstrating the need for researchers utilizing impulse facilities for hypervelocity boundary-layer instability and transition research to operate the facility in a manner least likely to introduce particulate to the test flow.

We compare FLDI (boundary-layer density disturbances) and heat transfer (surface mounted heat-transfer thermocouples) results before and after a stringent cleaning regimen was implemented. Prior to the implementation of the cleaning regimen, unpredictable turbulent spots were observed in both FLDI and thermocouple data at locations uncharacteristic of natural transition; we believe that it is likely these turbulent spots are the result of bypass transition initiated by particulate striking the model surface.

A statistical analysis of the correlation of tunnel parameters to transition location indicates that the coefficient of determination was significantly increased after the implementation of the clean-

Table 3. Multivariable linear regression analyses with Re_{Tr} (R^2 = 0.80) and Re^*_{Tr} (R^2 = 0.86) as the response variables for "clean" tunnel results (n = 34) acquired after the implementation of the new cleaning regimen. The coefficients found to be statistically significant ($p < 0.05$) are in bold print.

	Re_{Tr}	Re^*_{Tr}
Re intercept	$\mathbf{1.83 \times 10^6}$	-1.08×10^5
p-value	6.86×10^{-5}	0.73991
Standard Error	3.99×10^5	3.23×10^5
$C_{P_{res}}$	$\mathbf{7.20 \times 10^4}$	$\mathbf{3.54 \times 10^4}$
p-value	2.30×10^{-10}	1.29×10^{-9}
Standard Error	7.84×10^3	6.34×10^3
$C_{h_{res}}$	$\mathbf{-2.01 \times 10^5}$	3.39×10^4
p-value	0.00718	0.55180
Standard Error	6.97×10^4	5.64×10^4
model F-statistic	61.9	95.1
model p-value	1.49×10^{-11}	5.94×10^{-14}

ing regimen. This increase in the coefficient of determination is consistent with more repeatable transition locations and flow quality. The new cleaning regimen makes it possible to systematically characterize transition locations on the test article in a repeatable manner by carefully selecting run conditions. R^2 values for Re_{Tr}, Re^*_{Tr}, and N factor increase significantly with the introduction of a more stringent cleaning procedure. This ability to repeat transition locations facilitates fundamental hypervelocity boundary-layer stability and transition research.

The measurement of the time and size distribution of particulate matter in shock tunnel experiments warrants further study, and could aid in future experimental-computational comparisons.

Acknowledgments

The authors would like to thank Bahram Valiferdowsi (Caltech) for help running T5, Ross Wagnild (Sandia National Laboratories) for help with the program to compute the run conditions, and Elizabeth Jewell (University of Michigan) for statistical advice. This work was an activity that was part of National Center for Hypersonic Laminar-Turbulent Research, sponsored by the "Integrated Theoretical, Computational, and Experimental Studies for Transition Estimation and Control" project, supported by the U.S. Air Force Office of Scientific Research and the National Aeronautics and Space Administration (FA9552-09-1-0341). Additionally, this work was part of the "Transition

Delay in Hypervelocity Boundary Layers by Means of CO_2/Acoustic Interactions" project, sponsored by the Air Force Office of Scientific Research (FA9550-10-1-0491). J. S. Jewell received additional support from the National Defense Science and Engineering Graduate Fellowship, the Jack Kent Cooke Foundation, and the National Research Council Research Associateship.

References

[1] Bushnell, D., "Notes on Initial Disturbance Fields for the Transition Problem," *Instability and Transition*, edited by M. Hussaini and R. Voigt, ICASE/NASA LaRC Series, Springer US, 1990, pp. 217–232.

[2] Schneider, S. P., "Effects of High-Speed Tunnel Noise on Laminar-Turbulent Transition," *Journal of Spacecraft and Rockets*, Vol. 38, No. 3, 2001, pp. 323–333.

[3] Schneider, S. P., "Hypersonic Laminar-Turbulent Transition on Circular Cones and Scramjet Forebodies," *Progress in Aerospace Sciences*, Vol. 40, No. 1-2, 2004, pp. 1–50.

[4] Schneider, S. P., "Development of Hypersonic Quiet Tunnels," *Journal of Spacecraft and Rockets*, Vol. 45, No. 4, 2008, pp. 641–664.

[5] Hofferth, J. W., Humble, R. A., Floryan, D. C., and Saric, W. S., "High-Bandwidth Optical Measurements of the Second-Mode Instability in a Mach 6 Quiet Tunnel," *Proceedings of 51st AIAA Aerospace Sciences Meeting Including the New Horizons Forum and Aerospace Exposition*, AIAA 2013-0378, Grapevine, Texas, 2013.

[6] Kocian, T. S., Perez, E., Oliviero, N. B., Kuehl, J. J., and Reed, H. L., "Hypersonic Stability Analysis of a Flared Cone," *Proceedings of 51st AIAA Aerospace Sciences Meeting Including the New Horizons Forum and Aerospace Exposition*, AIAA 2013-0667, Grapevine, Texas, 2013.

[7] Stetson, K. F. and Rushton, G. H., "Shock Tunnel Investigation of Boundary-Layer Transition at M = 5.5," *AIAA Journal*, Vol. 5, No. 5, 1967, pp. 899–906.

[8] Mee, D. J., "Boundary-layer transition measurements in hypervelocity flows in a shock tunnel," *AIAA Journal*, Vol. 40, No. 8, 2002, pp. 1542–1548.

[9] Holden, M. S., Wadhams, T. P., and Candler, G. V., "Experimental Studies in the LENS Shock Tunnel and Expansion Tunnel to Examine Real-Gas Effects in Hypervelocity Flows," *42nd AIAA Aerospace Sciences Meeting and Exhibit*, AIAA 2004-0916, Reno, Nevada, 2004.

[10] Wadhams, T. P., Mundy, E., MacLean, M. G., and Holden, M. S., "Ground test studies of the HIFIRE-1 transition experiment, Part 1: Experimental results," *Journal of Spacecraft and Rockets*, Vol. 45, No. 6, 2008, pp. 1134–1148.

[11] MacLean, M., Wadhams, T., Holden, M., and Johnson, H., "Ground test studies of the HIFiRE-1 transition experiment, Part 2: Computational analysis," *Journal of Spacecraft and Rockets*, Vol. 45, No. 6, 2008, pp. 1149–1164.

[12] Tanno, H., Komura, T., Sato, K., Itoh, K., Takahashi, M., and Fujii, K., "Measurements of Hypersonic Boundary Layer Transition on Cone Models in the Free-Piston Shock Tunnel HIEST," *47th AIAA Aerospace Sciences Meeting including The New Horizons Forum and Aerospace Exposition*, AIAA 2009-0781, AIAA, Orlando, Florida, 2009.

[13] Fujii, K., Noriaki, H., Tadao, K., Shoichi, T., Muneyoshi, N., Yukihiro, I., Akihiro, N., and Hiroshi, O., "A Measurement of Instability Wave in the Hypersonic Boundary Layer on a Sharp Cone," *41st AIAA Fluid Dynamics Conference and Exhibit,* AIAA-2011-3871, Honolulu, Hawaii, 2011.

[14] Laurence, S. J., Wagner, A., Hannemann, K., Wartemann, V., Lüdeke, H., Tanno, H., and Itoh, K., "Time-Resolved Visualization of Instability Waves in a Hypersonic Boundary Layer," *AIAA Journal*, Vol. 50, No. 6, 2012, pp. 243–246.

[15] Laurence, S., Wagner, A., and Hannemann, K., "Schlieren-based techniques for investigating instability development and transition in a hypersonic boundary layer," *Experiments in Fluids*, Vol. 55, No. 8, 2014.

[16] Laurence, S. J., Wagner, A., Ozawa, H., Schramm, J. M., and Hannemann, K., "Visualization of a hypersonic boundary-layer transition on a slender cone," *19th AIAA International Space Planes and Hypersonic Systems and Technologies Conference*, AIAA-2014-3110, Atlanta, Georgia, 2014.

[17] Germain, P. D. and Hornung, H. G., "Transition on a Slender Cone in Hypervelocity Flow," *Experiments in Fluids*, Vol. 22, 1997, pp. 183–190.

[18] Adam, P. H. and Hornung, H. G., "Enthalpy Effects on Hypervelocity Boundary-layer Transition: Ground Test and Flight Data," *Journal of Spacecraft And Rockets*, Vol. 34, No. 5, 1997, pp. 614–619.

[19] Rasheed, A., Hornung, H. G., Fedorov, A. V., and Malmuth, N. D., "Experiments on Passive Hypervelocity Boundary-layer Control Using an Ultrasonically Absorptive Surface," *AIAA Journal*, Vol. 40, No. 3, MAR 2002, pp. 481–489.

[20] Jewell, J. S., Wagnild, R. M., Leyva, I. A., Candler, G. V., and Shepherd, J. E., "Transition Within a Hypervelocity Boundary Layer on a 5-Degree Half-Angle Cone in Air/CO_2 Mixtures," *51st AIAA Aerospace Sciences Meeting including the New Horizons Forum and Aerospace Exposition*, AIAA-2013-0523, Grapevine, Texas, 2013.

[21] Parziale, N. J., Shepherd, J. E., and Hornung, H. G., "Differential Interferometric Measurement of Instability in a Hypervelocity Boundary Layer," *AIAA Journal*, Vol. 51, No. 3, 2013, pp. 750–754.

[22] Fedorov, A. V., "Receptivity of a supersonic boundary layer to solid particulates," *Journal of Fluid Mechanics*, Vol. 737, 2013, pp. 105–131.

[23] Jewell, J. S., Parziale, N. J., Leyva, I. A., Shepherd, J. E., and Hornung, H. G., "Turbulent Spot Observations within a Hypervelocity Boundary Layer on a 5-degree Half-Angle Cone," *Proceedings of 42nd AIAA Fluid Dynamics Conference and Exhibit*, AIAA-2012-3062, New Orleans, Louisiana, 2012.

[24] Parziale, N. J., *Slender-Body Hypervelocity Boundary-Layer Instability*, Ph.D. thesis, California Institute of Technology, 2013.

[25] Parziale, N. J., Shepherd, J. E., and Hornung, H. G., "Free-stream density perturbations in a reflected-shock tunnel," *Experiments in Fluids*, Vol. 55, No. 2, 2014, pp. 1–10.

[26] Jewell, J. S., *Boundary-Layer Transition on a Slender Cone in Hypervelocity Flow with Real Gas Effects*, Ph.D. thesis, California Institute of Technology, Pasadena, CA, 2014.

[27] Parziale, N. J., Shepherd, J. E., and Hornung, H. G., "Observations of hypervelocity boundary-layer instability," *Journal of Fluid Mechanics*, Vol. 781, 2015, pp. 87–112.

[28] Gronvall, J. E., Johnson, H. B., and Candler, G. V., "Boundary-Layer Stability Analysis of High Enthalpy Shock Tunnel Transition Experiments," *Journal of Spacecraft and Rockets*, Vol. 51, 2014, pp. 455–467.

[29] Hornung, H. G., "Performance Data of the New Free-Piston Shock Tunnel at GALCIT," *Proceedings of 17th AIAA Aerospace Ground Testing Conference*, AIAA 1992-3943, Nashville, TN, 1992.

[30] Goodwin, D. G., "An Open-Source, Extensible Software Suite for CVD Process Simulation," *Proceedings of CVD XVI and EuroCVD Fourteen, M Allendorf, F Maury, and F Teyssandier (Eds.)*, 2003, pp. 155–162.

[31] Browne, S., Ziegler, J., and Shepherd, J. E., "Numerical Solution Methods for Shock and Detonation Jump Conditions," GALCIT - FM2006-006, 2006.

[32] Gordon, S. and McBride, B., "Thermodynamic Data to 20000 K for Monatomic Gases," NASA TP-1999-208523, 1999.

[33] McBride, B. J., Zehe, M. J., and Gordon, S., "NASA Glenn Coefficients for Calculating Thermodynamic Properties of Individual Species," NASA TP-2002-211556, 2002.

[34] Johnson, H. B., *Thermochemical Interactions in Hypersonic Boundary Layer Stabity*, Ph.D. thesis, University of Minnesota, Minnesota, 2000.

[35] Johnson, H. B., Seipp, T. G., and Candler, G. V., "Numerical Study of Hypersonic Reacting Boundary Layer Transition on Cones," *Physics of Fluids*, Vol. 10, No. 13, 1998, pp. 2676–2685.

[36] Wagnild, R. M., *High Enthalpy Effects on Two Boundary Layer Disturbances in Supersonic and Hypersonic Flow*, Ph.D. thesis, University of Minnesota, Minnesota, 2012.

[37] Taylor, J. R. and Hornung, H. G., "Real gas and wall roughness effects on the bifurcation of the shock reflected from the end wall of a tube," *Proceedings of the 13th International Symposium on Shock Waves*, ISSW, Niagara Falls, New York, USA, 1981.

[38] Davies, L. and Wilson, J. L., "Influence of Reflected Shock and Boundary-Layer Interaction on Shock-Tube Flows," *Physics of Fluids*, Vol. 12, No. 5, 1969, pp. I37.

[39] Smeets, G., "Laser Interferometer for High Sensitivity Measurements on Transient Phase Objects," *IEEE Transactions on Aerospace and Electronic Systems*, Vol. AES-8, No. 2, 1972, pp. 186–190.

[40] Wilkinson, S. P., Anders, S. G., Chen, F.-J., and Beckwith, I. E., "Supersonic and Hypersonic Quiet Tunnel Technology at NASA Langley," *17th Aerospace Ground Testing Conference*, AIAA 1992-3908, Nashville, Tennessee, 1992.

[41] Sanderson, S. R., *Shock wave interaction in hypervelocity flow*, Ph.D. thesis, California Institute of Technology, Pasadena, CA, 1995.

[42] Sanderson, S. R. and Sturtevant, B., "Transient heat flux measurement using a surface junction thermocouple," *Review of Scientific Instruments* , Vol. 73, No. 7, 2002, pp. 2781–2787.

[43] Jewell, J. S. and Shepherd, J. E., "T5 Conditions Report: Shots 2526–2823," Tech. rep., California Institute of Technology, Pasadena, CA, June 2014, GALCIT Report FM2014.002.

[44] Draper, N. R. and Smith, H., *Applied Regression Analysis*, John Wiley & Sons, London, 1998.

[45] MathWorks, MATLAB v. 8.1.0.604 (R2013a), `LinearModel` documentation page, http://www. mathworks.com, 2013.

[46] Jewell, J. S., Shepherd, J. E., and Leyva, I. A.,"Shock tunnel operation and correlation of boundary layer transition on a cone in hypervelocity flow," *Proceedings of the 29th International Symposium on Shock Waves*, ISSW29-000300, Madison, Wisconsin, 2013.